Kapal: Jurnal Ilmu Pengetahuan dan Teknologi Kelautan
(Kapal: Journal of Marine Science and Technology)
journal homepage : http://ejournal.undip.ac.id/index.php/kapal
2301-9069 (e)
1829-8370 (p)

Influence of Stress Concentration Factor due to Scallop Form on the Wrang Plate Structure

Riska Arum Dona Kusnadi Putri[1)], Totok Yulianto[1)*)], Rizky Chandra Ariesta[1)], Mohammad Nurul Misbah[1)]

[1)] Department of Naval Architecture, Faculty of Marine Technology, Sepuluh Nopember Institute of Technology, Surabaya 60111, Indonesia
[*)] Corresponding Author: totoky@na.its.ac.id

Article Info

Keywords:
Scallop;
Concentration;
Finite Element Analysis (FEA);
Structure

Article history:
Received: 14/12/2021
Last revised: 06/03/2022
Accepted: 07/03/2022
Available online: 07/03/2022
Published: 07/03/2022

DOI:
https://doi.org/10.14710/kapal.v19i3.43344

Abstract

As one of the ship structures, scallops are applied to reduce the stress concentration around the joint of a plate with stiffeners or girder. The current implementation of scallops is usually ordinarily formed following the profile. Stress concentration occurs, which causes hotspot, crack, and failure conditions to the structures because of loads, which can be solved more optimally by optimizing scallops design. In this research, numerical models will be performed by finding the optimum scalloped shapes. The variations of three provided scallops geometry, such as model (1), model (2), and model (3), are compared to obtain the optimized stress reduction result analyzed. Numerical simulations are performed using Finite Element Analysis (FEA), based on the FE method with the ANSYS student version. Compared to all the models, in this case, comparative values of the scallops models are found that the smaller stress concentration result, the most optimal model. The scallop model (2) has produced the smallest stress concentration. Therefore, it can be concluded that model (2) is the most optimal scallop for intersection in wrang plate structure.

1. Introduction

The scallop is one of the ship structures detailed to through stiffener, girder, and to prevent stress concentration occurs caused by loads. The conventional form of scallops is normally applied in whole parts of web frames. The scallops are appertaining minor structure also need to optimization to obtain the greatest performance for preventing stress concentration. Besides that, it found that there are several forms of the scallops, that geometry and dimension influence the resistance power of stress, crack, and fatigue is analyzed [1], [2]. All the ships especially merchant ships are using structural details to reduce stress concentrations in numerous parts of the structure.

In the shipbuilding process, the plate is the primary resource of construction. The construction will serve into a variety of panels, from that panel assembly into a block, and running becomes a ship. Any holes were generated for a few purposes like manholes, dry holes, doors, windows, and scallops [3]. However, opening in ship structure has opportunities for vulnerability because of cyclic loads. Then, in terms of ship structural details need analysis satisfactorily. Strength analysis can prove that construction is strong enough, i.e., shaft strength calculations are performed using the finite element method until stress and deformation area is shown [4].

The finite element analysis (FEA) for strength assessment has been provided by several researchers. Most scientists have usually been conducted to evaluate numerous geometric forms of construction to obtain the best configuration. Moreover, Ismail [5] investigated the stress and deformation due to wave pressure acting on the side shell of a tanker ship using finite element analysis (FEA). Yulianto [6] conducted a numerical study of a lashing rod for a container and optimize the size with joint bolt interactions force. Additionally, the review from [7]-[10] conducted a numerical analysis of ship structure. The analysis showed that a new configuration of ship construction reduces the stress and deformation.

Moreover, based on the previous research, there is no identification according to the optimal geometry of scallops using several types of models in the wrang structure. Therefore, this research aims to develop scallop geometry models by optimizing the stress concentration due to load. In the analysis, a numerical study is performed by the FEM method using Finite Element Analysis Software. The FEA model modification will be discussed in detail in the next segment. The research is expected to enhance ship structure details in Indonesia's shipbuilding.

2. Methods

2.1. Research Process

The research process is normally illustrated in the flow diagram shown in Fig. 1 and will be informed in detail by degrees.

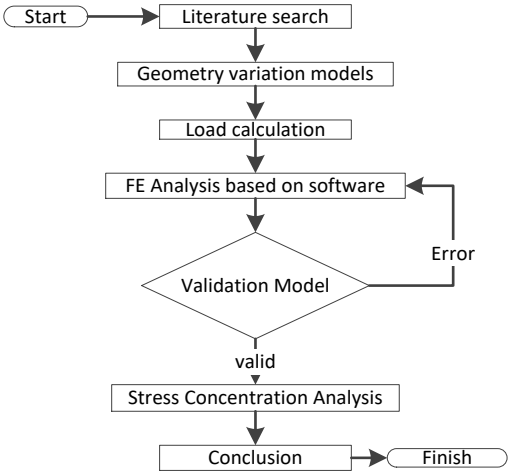

Figure 1. Research Flow Process.

In the current study, the finite element analysis is used by performing the finite element method implementation. The variation of analysis is wrang plate geometry of bottom tanker ship, the variations model is shown in Fig. 2.

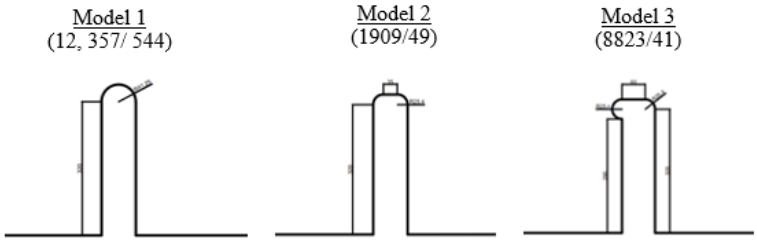

Figure 2. Developed Scallop Forms of Wrang Plate.

2.2. Modeling

From Fig. 1, the model is represented in the wrang plate that is apart from the bottom construction. Each inner bottom and bottom are subject to different loading conditions, the inner bottom is loaded by inner pressure from the cargo, and the bottom is loaded by hydrostatic pressure. The inner pressure tank is determined using the Eq. 1 [11]:

$$P_{in-tk} = \rho\, g\, z_{tk} \tag{1}$$

P_{in-tk} is tank static pressure in kN/m^2, ρ density of the liquid in the tank in t/m^3, g acceleration due to gravity in m/s^2 and z_{tk} is the vertical distance from the hi-point of the tank. And the hydrostatic load can be shown in Eq. 2 as follow [11]:

$$P_{hys} = \rho_{sw}\, g\, (T_{LC} - z) \tag{2}$$

P_{hys} is sea static pressure, ρ_{sw} seawater density in t/m^3, T_{LC} draft in the loading condition being considered in m, and z is the vertical coordinate of the load point in m. From Eq. 1 and 2 above, the load value for the inner bottom and bottom is obtained. The load numbers experienced for the areas model are shown in Table 1.

Table 1. Data of load per unit area

Load	Pressure (MPa)
tank static pressure	12.88
Sea static pressure	11.73

Furthermore, the mechanical properties of the material for the model are summarized in Table 2.

Table 1 Mechanical Properties A36

Description	Size	Unit
Density	7850	ton
Young's modulus	200	GPa
Poisson's ratio	0.26	
Shear modulus	79.3	GPa
Bulk Modulus	140	GPa
Compressive Yield Strength	152	MPa
Tensile Strength, Yield	250	MPa
Tensile Strength, Ultimate	400	MPa

Based on the ship data, the model was assumed to use a wrang plate and a double bottom panel as shown in Fig. 3. The dimensions of the model are 3600 x 3000 x 1850 mm, with a frame spacing of 600 mm. Moreover, the thickness of the inner bottom plate and the bottom plate are 12 mm, the side girder 11 mm, and the wrang plate 12 mm. The profile applied in the model is the same, especially using the bulb profile with dimensions 320 x 12 mm.

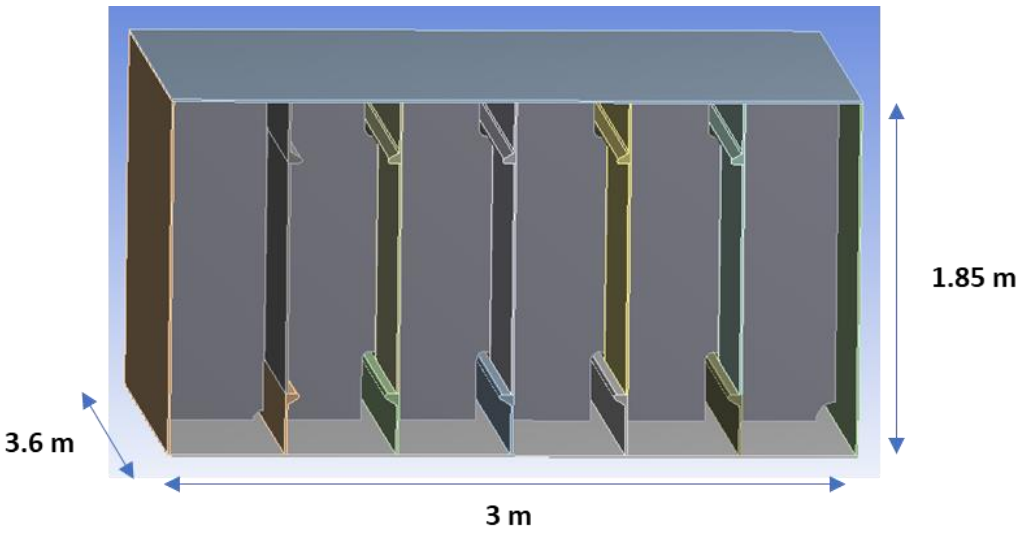

Figure 3. Global model for transfer load

From the model above, for analysis model will focus on the inside wrang plate the model illustrates in Fig. 4.

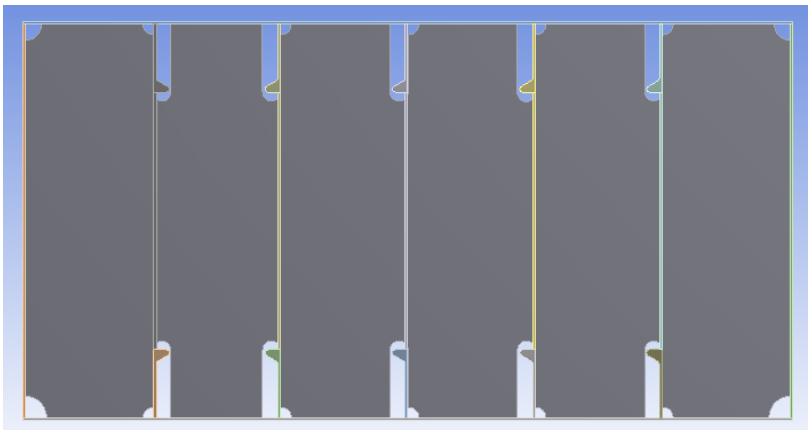

Figure 4. Model wrang plate

2.3. Boundary Condition

Boundary conditions are used in the one of edge the model, it represents the girder of the ship, also all edges are free in order to be near a real condition of the structure. Fixed support is installed on the center girder and side girder. However, If there are interacting geometries, the surfaces of those geometries must be ensured to be connected. In addition, a gap check is carried out, to ensure whether there are overlapping geometries or even unwanted gaps between geometries. The boundary condition is represented in Fig. 5.

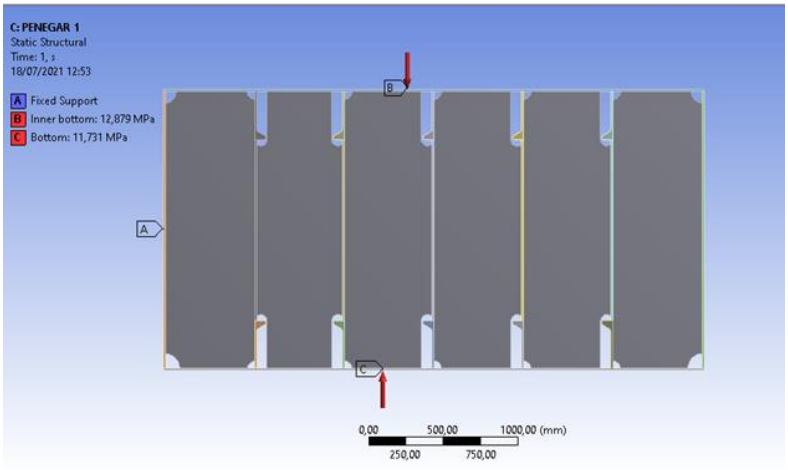

Figure 5. Boundary Conditions model.

2.4. Meshing Model

The meshing stage was used to describe the geometry area. The specific mesh will be more accurate, but the cache files will be bigger, and time-consuming for the time simulation. Bottom pane structure modeling used Hexa elements with approximately more stability to reach convergency for analyzed [9]. The model meshing is represented in Fig. 6.

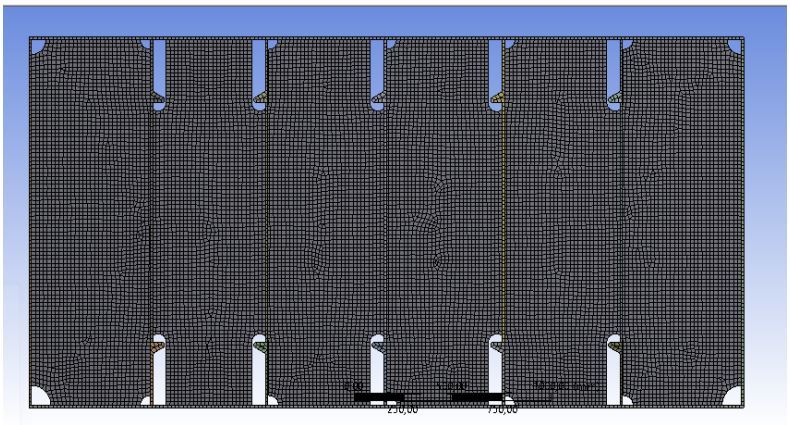

Figure 6. Meshing Structure Wrang Plate Model with structural mesh.

Furthermore, to determine the stress concentration factor by dividing the maximum stress between the model by the nominal stress, with the following Eq. 3 as follows [12]:

$$\mathrm{Kt} = \frac{\sigma_{max}}{\sigma_{nom}} \tag{3}$$

From the formula above, the maximum stress of each model is known, so to get the stress concentration factor, it is necessary to first find the nominal stress. The nominal stress is the total stress in an element under uniform loading conditions in the absence of concentrated stress. The nominal stress can be obtained by placing the coordinates in the center of the model that is not affected by the presence of holes.

3. Results and Discussion

3.1. Convergence Study

A convergence study is one way to determine the correct size of elements in modeling to produce a stable result that shown in Table 3 and Fig. 7. Meshing was done using the Hexa element method [9], [13], [14]. Wrang structure is convergence in the mesh size of 20 mm, therefore that mesh is used for all analysis.

Table 3. Element size and Error in Convergence

element size (mm)	Number of element	Stress (Mpa)	Error (%)
100	2328	474.57	
90	2467	427.22	11.08
80	2613	510.81	16.36
70	2370	514.37	0.69
60	3379	367.81	39.85

element size (mm)	Number of element	Stress (Mpa)	Error (%)
50	3140	384.31	4.29
40	4742	514.37	25.29
30	7707	518.18	0.74
20	17367	511.12	1.38

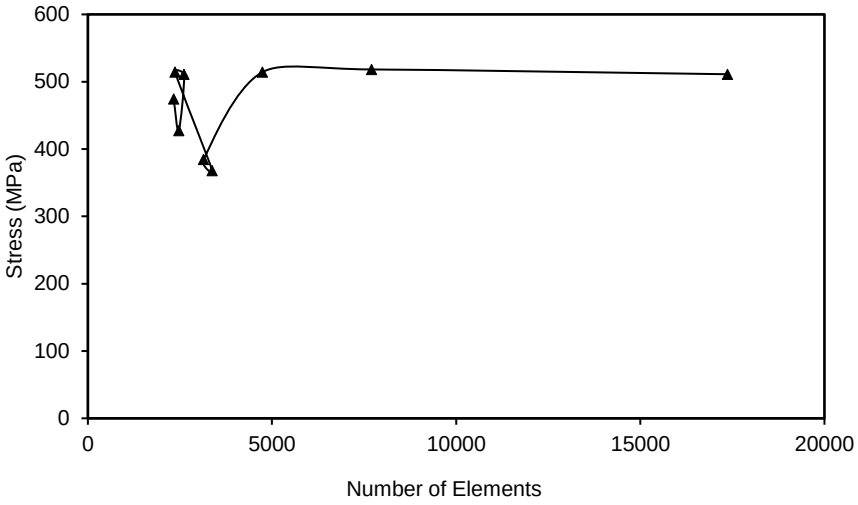

Figure 7. Convergence Study

3.2. Determine Stress Concentration Factor on Scallop in Wrang Structure

The analysis is carried out when all the requirements have been obtained, like as: have reached convergence on meshing, obtained stress values on the several variations model. To determine the stress concentration factor, need to choose point stress data on the element of the model. First, the finite element model generates to obtain responses to stress in several components, such as stress distribution X, Y, and Z directions. To obtain stress concentration factor is needed to make a new point in the scallop for reach data of concentrated force and the middle plate for nominal stress. The profile is numbered from left to right starting from 1 until 5, and the inner bottom (up) gives the notation IB, and the bottom (below) marking with B. The illustration of the numbering result it can be shown in Fig. 8.

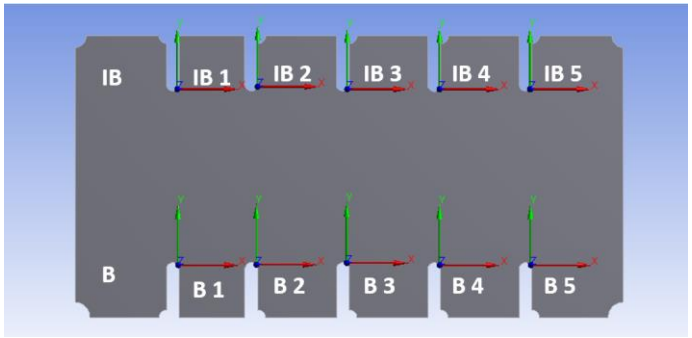

Figure 8. Notation for scallop model arrangements.

Furthermore, the contour from the simulation is represented in Fig. 9 – Fig. 11.

Normal Stress (a)

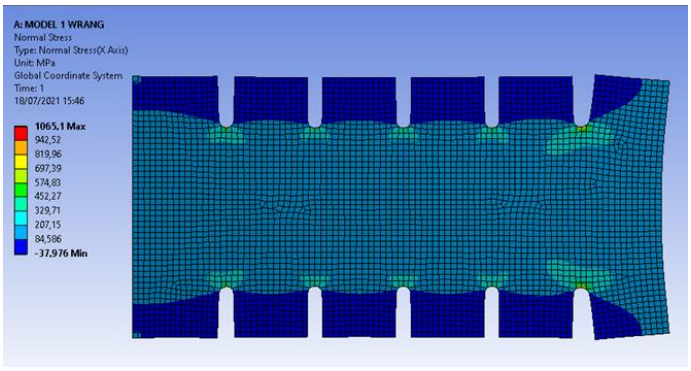

Concentrated Stress (b)

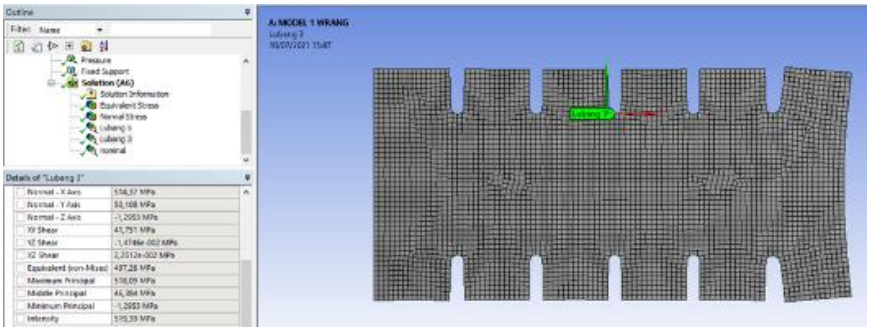

Nominal Stress (c)

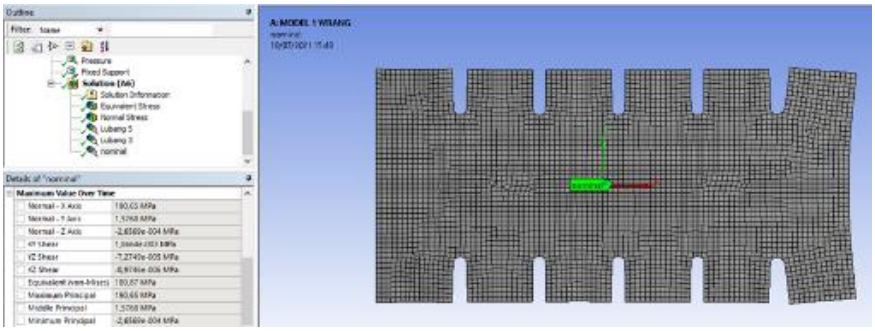

Figure 9. Contour Stress Model 1

Normal Stress (a)

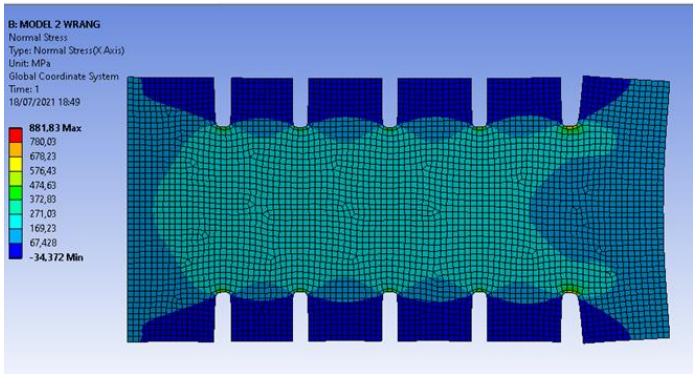

Concentrated Stress (b)

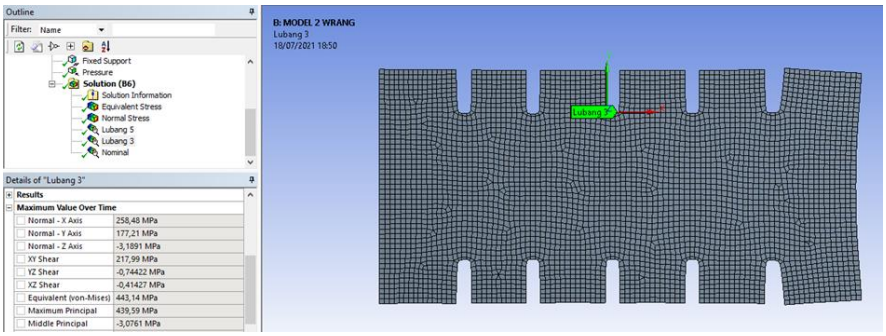

Nominal Stress (c)

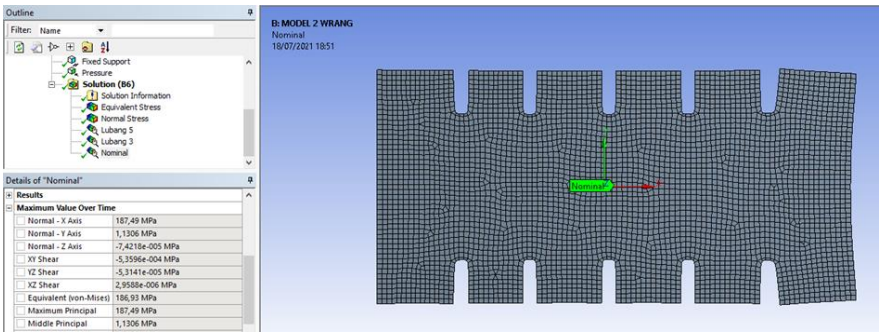

Figure 10. Contour Stress Model 2

Normal Stress (a)

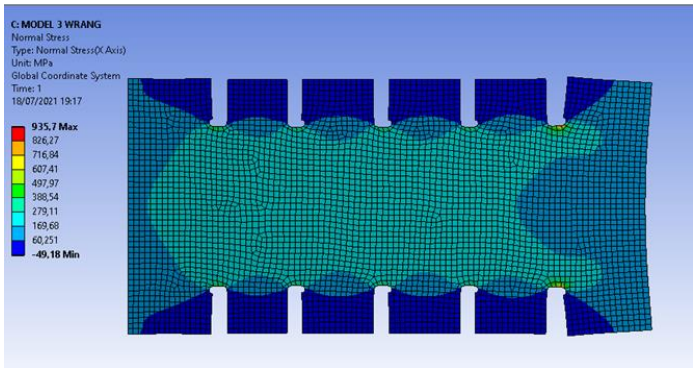

Concentrated Stress (b)

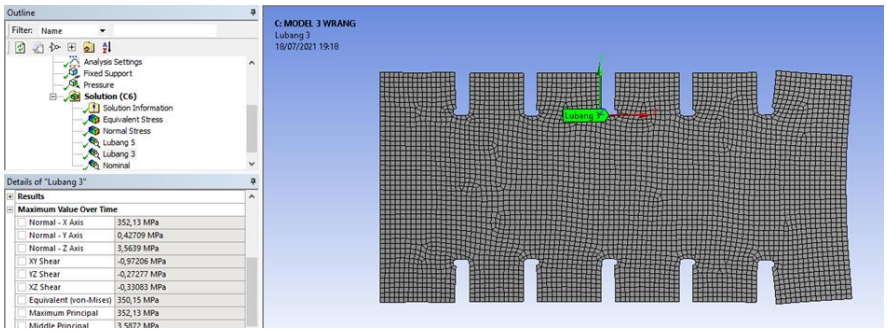

Nominal Stress (c)

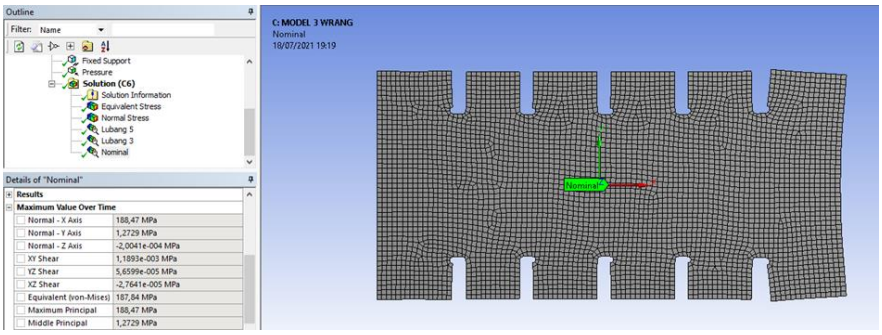

Figure 11. Contour Stress Model 3.

Based on the results of the analysis carried out, it can be displayed in tabular form in Table 4 can be seen the value of nominal stress, concentrated stress, and stress concentration factor value.

Table 4. Recapitulation of Stress and SCF of Each Model

Variation	Concentrated stress (MPa)	Nominal Stress (MPa)	Stress Concentration Factor
Model I	135.45	50,197	2.698
Model II	98.473	45.896	2.145
Model III	103.14	45.253	2.280

Based on the table above, the highest stress concentration factor is owned by model I, which is 2.698. The lowest SCF value is 2.145 in model II. The difference between nominal stress and concentrated stress certainly affects the stress concentration factor. The difference in SCF value is influenced by the existing hole geometry. The sharper the curve of the discontinuity, the greater the stress concentration. Of the three types of scallop models used, the model I has a simple model but the curve is too steep, resulting in concentrated stress. Geometry models II and III use a combination of local shapes, circles, and straight lines. This causes the stress flow to change smoothly from a uniform state to then adjust the geometry of the model.

3.3. Wrang Plate Stress Concentration Factor Validation

Model validation is an activity to compare the results obtained from the process using the software finite element analysis with the empirical formula obtained from the literature review in the previous chapter. This formula can estimate the stress concentration factor with a difference of 2% from the photoelastic experimental results that it has good validity to determine whether the software simulation results are acceptable or not by comparing the numerical results with the empirical results. The concepts were applied in laboratory-scale experiments to obtain stress concentration factors in a good agreement result [15,16]. The graph of empirical results can be seen in Figure 12.

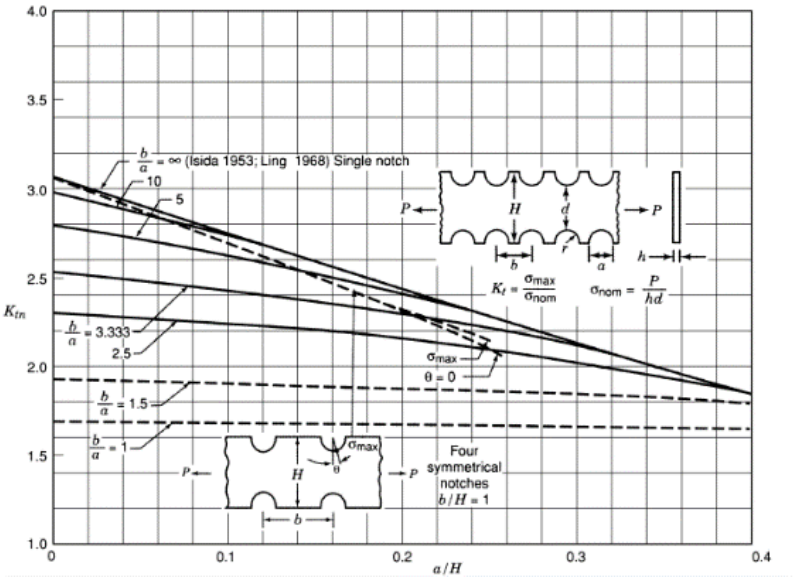

Figure 12. Stress Concentration Factor Graph [17]

The calculation and comparison of stress concentration factors can be seen in Table 5. From the calculation, the stress concentration factor value with the graph is 2.727 while the stress concentration factor value using finite elements is 2.69. So that the difference between the empirical method and the finite element is 1.065%.

Table 5. Empirical Comparison with Numerical

Calculation Empirical SCF	Calculation Numerical SCF	Difference (%)
b/a = 7.272 a/H = 0.044	max =135.45 nom =50,197	1.065
SCF = 2.727	SCF = 2.69	

3.4. Stress Concentration Factor on Wrang Plate Panel

The value of the stress concentration factor or stress concentration factor in failure mode I with the boundary conditions in this study, the stress used is the normal stress in the X-axis direction as shown in Fig. 13.

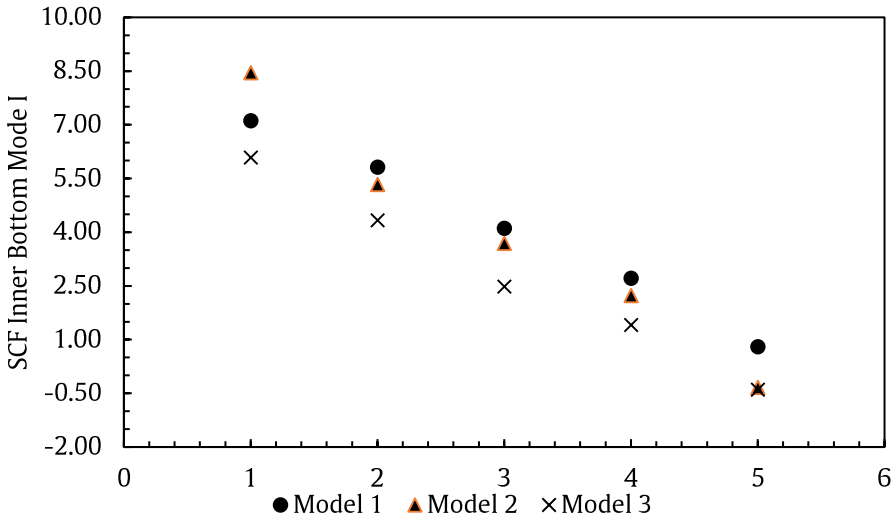

Figure 13. Inner Bottom Graph Mode I

Based on Fig. 13, it can be concluded that model III has the lowest SCF value compared to the other two models. The highest SCF value in Mode I for the inner bottom in model II at point B1 is 8.453. While the lowest SCF is 0.340 in model II at point B5 illustrated in Fig. 14.

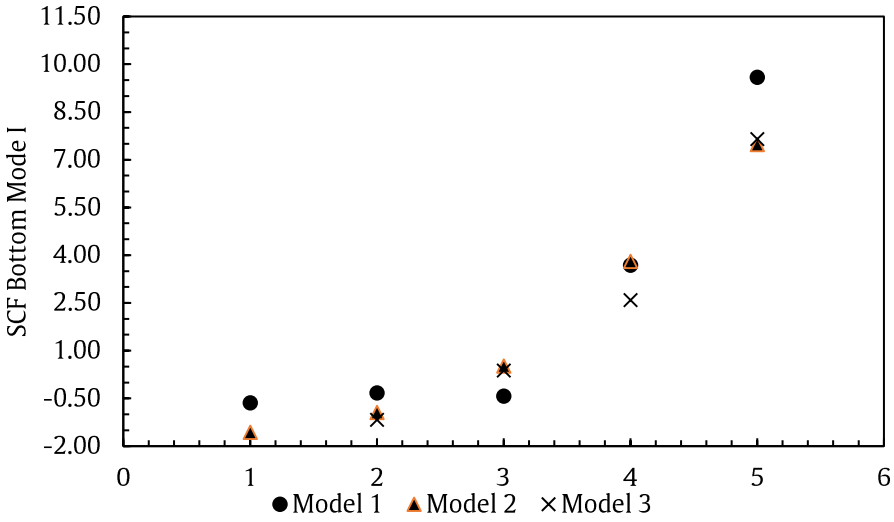

Figure 14. SCF Bottom Graph Mode I

The highest SCF value in model I is 9.588 in model I point B5 while the lowest SCF value of 0.340 in model II point B3.

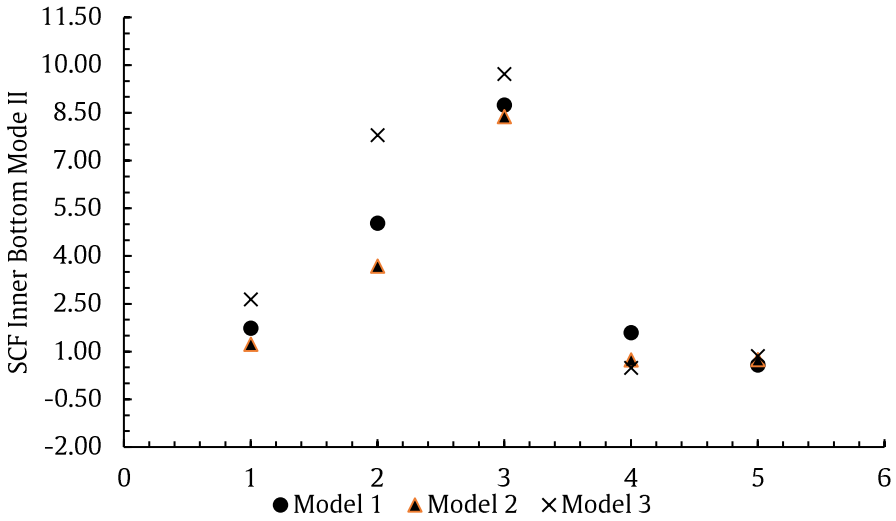

Figure 15. SCF Inner Bottom Graph Mode II

In the SCF Inner bottom graph, it can be seen that all models experience the same trend, namely increasing from point IB 1 to IB 3, then decreasing at IB 4 and IB 5 in Fig. 15. it can be seen that the highest SCF value of Moda II on the inner bottom is located at the IB3 Model III point, which is 9.715. While the lowest SCF value of Mode II on the inner bottom is located at the IB4 Model III point, 0.482.

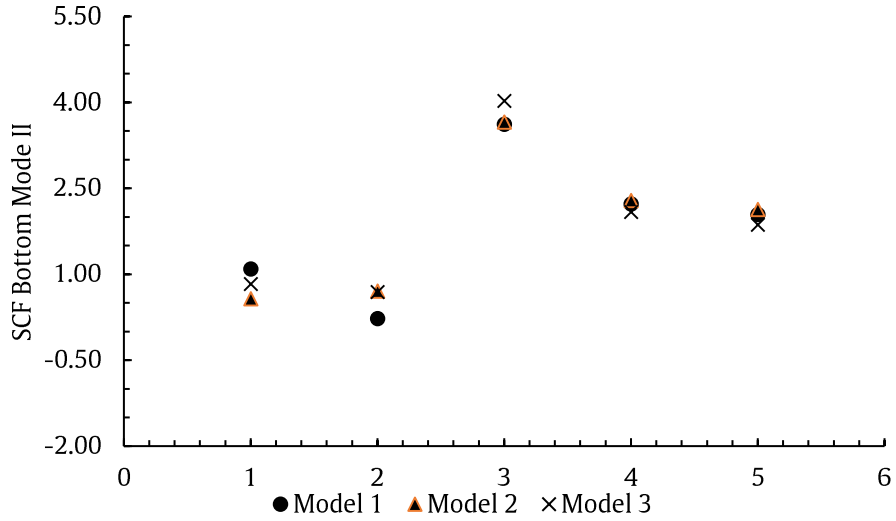

Figure 16. SCF Bottom Graph Moda II

From Fig. 16, it can be concluded that the highest SCF value in mode II 4.027 lies in model III point B3 while the lowest SCF value of 0.229 lies in a model I point B2.

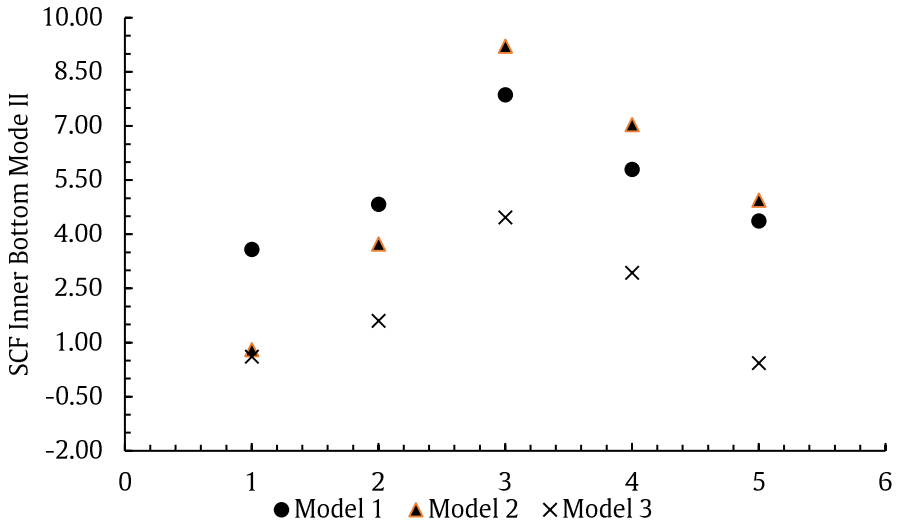

Figure 17. SCF Inner Bottom Graph Mode III

In the SCF Inner bottom graph, it can be seen that all models experience the same trend, namely increasing from point IB 1 to IB 3, then decreasing at IB 4 and IB 5. In Fig. 17, it can be seen that the highest SCF value of Mode III on the inner bottom is located at the IB3 Model II point, which is 9.715. While the lowest SCF value of Mode III on the inner bottom is located at the IB5 Model III point, which is 0.482.

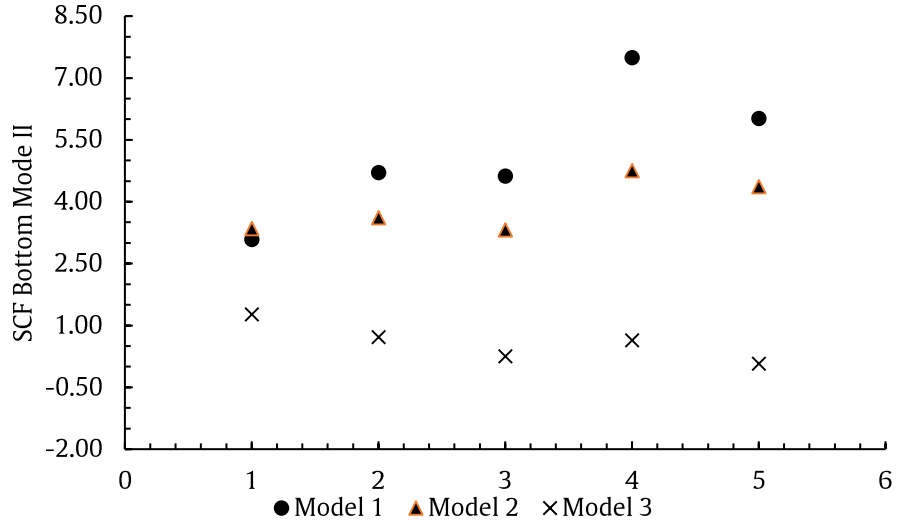

Figure 18. SCF Bottom Graph Mode III

Fig. 18 shows that the highest SCF value in mode III is 7.491, located on a model I point B4, while the lowest SCF value is 0.074 on model III point B5. All SCF data will be recapitulated and averaged into one in Table 6.

Table 6. Recapitulation of the average value of SCF for each Mode

Place	Model	SCF Mode 1	SCF Mode 2	SCF Mode 3
IB	I	4.109	3.535	5.285
	II	4.007	2.956	5.145
	III	2.937	4.298	2.005
B	I	2.934	1.842	5.185
	II	2.861	1.872	3.879
	III	2.831	1.900	0.591

Based on the panel model analysis it can be concluded that model III has the smallest stress concentration factor value in case modes I and III but for mode II the smallest stress concentration factor value in model II. This is due to the combination of geometries in the scallop model to make the stress flow smooth [18]. The combination of experimental and numerical can be provided in future research to obtain comparison results.

4. Conclusion

After analyzing the data, the following conclusions were obtained:

1. In the bottom panel model with inner bottom and bottom static loads, the stress concentration factor values are as follows:
   - Model I produces stress concentration factor values in mode I of 4.109 (inner bottom) and 2.934 (bottom), in mode II of 3.535 (inner bottom) and 1.842 (bottom), and mode III of 5.285 (inner bottom) and 5.185 (bottom).
   - Model II produces stress concentration factor values in mode I of 4,007 (inner bottom) and 2,861 (bottom), in mode II of 2,956 (inner bottom) and 1,872 (bottom), and mode III of 5,145 (inner bottom) and 3,879 (bottom).
   - Model III produces stress concentration factor values in mode I of 2,937 (inner bottom) and 2,831 (bottom), mode II of 4,298 (inner bottom) and 1,900 (bottom), and mode III of 2,005 (bottom) and 0,591 (inner bottom).
2. Based on the analysis of the panel model, it can be concluded that model III has the smallest stress concentration factor value in cases of mode I and III but for mode II the smallest stress concentration factor value in model II.

Acknowledgments

The authors thank colleagues in Institut Technology of Sepuluh Nopember, specifically in the Naval Architecture department, for all the guidance and insight to the author during the process of this research.

References

[1] H. W. Leheta, A. M. H. Elhewy, and H. A. Younes, " Analysis Of Fatigue Crack Growth In Ship Structural Details," *Polish Maritime Research*, vol. 23, no. 2, pp. 71– 82, 2016, doi: 10.1515/pomr-2016-0023

[2] S. H. Sujiatanti, T. Yulianto, W. H. A. Putra, and R. C. Ariesta, " Influence of the Cut-out Shape on the Fatigue Ship Structural Detail," Proceedings of the 6th International Seminar on Ocean and Coastal Engineering, Environmental and Natural Disaster Management (ISOCEEN 2018), pp. 111– 115, 2020, doi: 10.5220/0008375601110115.

[3] M. Nurul Misbah, S. Hardy Sujiatanti, D. Setyawan, R. Chandra Ariesta, and S. Rahmadianto, " Structural analysis on the block lifting in shipbuilding construction process," *MATEC Web Conference*, vol. 177, pp. 1– 6, 2018, doi: 10.1051/matecconf/201817701027.

[4] T. Yulianto and R. C. Ariesta, " Analisis Kekuatan Shaft Propeller Kapal Rescue 40 Meter dengan Metode Elemen Hingga," *Kapal: Jurnal Ilmu Pengetahuan dan Teknolologi Kelautan*, vol. 16, no. 3, pp. 100– 105, 2019, doi: 10.14710/kapal.v16i3.23572.

[5] A. Ismail, A. Zubaydi, B. Piscesa, T. Tuswan, and R. C. Ariesta, " Study Of Sandwich Panel Application On Side Hull Of Crude Oil Tanker," *Journal of Applied Engineering Science*, 2021, doi: 10.5937/jaes0-30373.

[6] T. Yulianto, S. H. Sujiatanti, R. C. Ariesta, and M. R. Aufar, " Strength Analysis of a Container Lashing on the Container Ship by Using Finite Element Method," Proceedings of the 6th International Seminar on Ocean and Coastal Engineering, Environmental and Natural Disaster Management (ISOCEEN 2018), pp. 101– 105, 2020, doi: 10.5220/0008375401010105.

[7] T. Tuswan, K. Abdullah, A. Zubaydi, and A. Budipriyanto, " Finite-element analysis for structural strength assessment of marine sandwich material on ship side-shell structure," in *Materials Today: Proceedings*, 2019, vol. 13, doi: 10.1016/j.matpr.2019.03.197.

[8] Misbah, M.; Setyawan, D.; Yulianto, T.; Ariesta, R. and Putra, W. (2022). Stress Concentration Analysis on Ship Plate with Hole using Numerical Approach. In Proceedings of the 4th International Conference on Marine Technology - senta, ISBN 978-989-758-557-9, pages 117-121. DOI: 10.5220/0010855200003261

[9] R. Ariesta and A. Chandra; Zubaydi, Achmad; Ismail, " Identifikasi Kerusakan pada Pelat Sandwich Lambung Sisi Menggunakan Metode Elemen Hingga," *Wave: Jurnal Ilmu Teknologi Maritim*, vol. 14, no. 2, pp. 83– 90, 2020. doi: 10.29122/jurnalwave.v14i2.4727

[10] A. I. Wulandari, N. W. D. Rahmasari, L. P. Adnyani, Alamsyah, R. J. Ikhwani" Fatigue Analysis of 5000 GT Ferry Ro-Ro' s Car Deck Using Finite Element Method," vol. 18, no. 3, pp. 160– 170, 2021, doi:10.14710/kapal.v18i3.39268.

[11] IACS, " Common Structural Rules for Double Hull Oil Tankers," IACS, 2012.

[12] W. C. Young and R. G. Budynas, *Roark's Formulas for Strain and Strain*, Seventh Ed., vol. 4, no. C. United States of America: McGraw-Hill, 2002.

[13] D. L. Logan, *A first course in the finite element method*, Fourth Edi. Canada: Chris Carson, 2007.

[14] K. K. Rumayshah, T. Dirgantara, H. Judawisastra, and S. Wicaksono, " Numerical micromechanics model of carbon fiber-reinforced composite using various periodical fiber arrangement," *Journal of Mechanical Science and Technology*, 2021, doi: 10.1007/s12206-021-0306-9.

[15] R. C. Ariesta, A. Zubaydi, A. Ismail, and T. Tuswan, " Identification of Damage Size Effect on Natural Frequency of Sandwich Material using Free Vibration Analysis," *Nase More*, vol. 69, no.1, pp. 1-8, 2022. doi: 10.17818/NM/2022/1.1.

[16] T. Tuswan, A. Zubaydi, B. Piscesa, A. Ismail, R. C. Ariesta, and A. R. Prabowo, " A numerical evaluation on nonlinear dynamic response of sandwich plates with partially rectangular skin/core debonding," *Curved Layered Structure*, vol. 9, no. 1, pp. 25– 39, 2022, doi: 10.1515/cls-2022-0003.

[17] W. D. Pilkey, *Peterson' s Stress Concentration Factors*. New York: John Wiley & Sons, Inc., 1997.

[18] Y. Takaki and K. Gotoh, " Approximate Weight Functions Of Stress Intensity Factor For A Wide Range Shapes Of

Surface And An Embedded Elliptical Crack," *Marine Structures*, vol. 70, pp. 102696, 2020, doi: 10.1016/j.marstruc.2019.102696.